PROCEEDINGS of the
23rd International Congress on Acoustics

9 to 13 September 2019 in Aachen, Germany

Prediction of the sound absorption of micro-perforated panels whose holes are extended in length by tubes

John Laurence DAVY[1]; Mohammad FARD[2]; Qian ZHANG[3]; Yadong LYU[4]; Jun YANG[5]

[1]Infrastructure Technologies, CSIRO, Australia & School of Science, College of Science, Engineering and Health, RMIT University, Australia

[2]School of Engineering, College of Science, Engineering and Health, RMIT University, Australia

[3, 4, 5]The Key Laboratory of Noise and Vibration Research, Institute of Acoustics, Chinese Academy of Sciences, China

ABSTRACT

Maa's theory, which models the specific acoustic impedance of a narrow air-filled hole in front of an air cavity using a lumped parameter model, works well for short holes at low frequencies. However, as the length of the hole or the frequency increases, the acoustic velocity of the air in the hole varies along the length of the hole as well as radially. It is necessary to use the transfer matrix method (TMM) rather than Maa's lumped parameter model to calculate the impedance of the hole and the cavity behind it. The peak sound absorption of a micro-perforated panel (MPP) in front of an air cavity can be moved to lower frequencies by extending the length the holes in the MPP with rigid or flexible tube bundles in the air cavity behind the MPP without increasing the total depth of the sound absorbing system. Previously Maa's lumped parameter model had been used to predict the sound absorption coefficients of these tube bundle sound absorbers. These predictions are only correct up to a certain frequency which depends on the length of the tube extended holes. This paper predicts the sound absorption to higher frequencies using the TMM.

Keywords: Sound, Absorption, Micro-perforated panel

1. INTRODUCTION

In order to obtain better sound absorption at low frequencies, in 2001 Lyu *et al.* (1) introduced the approach of extending the length of holes in a perforated panel in front of an air cavity by attaching tubes in the air cavity with the same or similar diameter to the back of the holes. In (1) and in several later papers, Lyu *et al.* presented experimental results of this approach and gave some theoretical formulae. However, they never actually published the results of any theoretical calculations. In 2011, Zhang (2) compared the theory with experimental results. Zhang followed the approach of Maa (3) and ignored wave motion along the length of the tubes. Zhang also ignored wave motion in the air cavity in the direction of cavity depth, although Maa had included it. This was presumably because the ends of the tubes opening into the air cavity were not usually at one edge of the air cavity. The ignoring of wave motion in the tubes and the air cavity meant, as Zhang commented, that her calculations would only be accurate when the wavelength of sound was greater than 10 times the length of the tubes and greater than 10 times the depth of the cavity. In 2016, Larner and Davy (4) pointed out that it was sometimes necessary to consider wave motion in the holes of the panel and/or the tubes at high frequencies even if the length of the hole was only 10 mm. When Davy was visiting the Institute of Acoustics of the Chinese Academy of Sciences (CAS) in 2018 under the CAS-CSIRO exchange scheme, he suggested that they repeat Zhang's calculations while taking account of wave motion in both the tubes and the air cavity. The comparisons of these new calculations with Zhang's

[1] john.davy@rmit.edu.au
[2] mohammad.fard@rmit.edu.au
[3] zhangqian3989@dingtalk.com
[4] yadong@mail.ioa.ac.cn
[5] jyang@mail.ioa.ac.cn

experimental results are reported in this paper. Lyu drew Davy's attention to the fact that Simon (5) had also made calculations taking account of wave motion in similar sound absorbing systems. Simon's theoretical modelling assumed that his tube ends opened into the air cavity at one end of air cavity, although this was not actually the case with his experimental measurements. In this paper, the position of the ends of the tubes where they open into the air cavity is considered. Simon also used formulae for the propagation of sound between two closely spaced plates rather than formulae for the propagation of sound in narrow tubes as used in this paper.

2. THEORY

In this paper, the time dependence of a pure tone wave is assumed to be proportional to $\exp(j\omega t)$. This choice effects the sign of the imaginary part of the impedances. The normalized specific acoustic impedance z_2 encountered by a plane sound wave incident normally on a planar layer of an acoustic medium on plane 2 of the two planes which bound the planar layer of the acoustic medium lying between the planes numbered 2 and 1 is (6)

$$z_2 = z_c \left[z_c \sin(kL) - jz_1 \cos(kL) \right] / \left[z_1 \sin(kL) - jz_c \cos(kL) \right]. \tag{1}$$

The acoustic medium has a normalized characteristic specific acoustic impedance of z_c and wave number of k. The distance between the two planes is L. The normalized specific acoustic impedance encountered by a plane wave incident normally on plane 1 from the acoustic medium is z_1. The specific acoustic impedances are normalized by dividing them by the characteristic specific acoustic impedance of the free acoustic medium $\rho_0 c_0$, where ρ_0 is the ambient density of the free acoustic medium and c_0 is the speed of sound in the free acoustic medium.

If z_1 tends to infinity, dividing the numerator and denominator of Eq. (1) by z_1, shows that Eq, (1) tends to

$$z_2 = -jz_c \cot(kL). \tag{2}$$

Eq. (2) will be used for a planar layer of an acoustic medium which is rigidly terminated at plane 1. It shows that a rigidly terminated planar layer of acoustic medium behaves like an acoustic spring at low frequencies. If $z_1 = 0$, Eq. (1) becomes

$$z_2 = jz_c \tan(kL). \tag{3}$$

Eq. (3) shows that a planar layer of an acoustic medium behaves like an acoustic mass at low frequencies if it is freely terminated at plane 1 by a large space or half space containing a similar acoustic medium. The open end of a hole or tube is a good approximation to free termination, although it is necessary to add a normalized specific acoustic impedance end correction to take account of the fact that the normalized specific acoustic impedance which the end of the hole or tube experiences is not completely zero.

For air in narrow circular holes or tubes, the normalized characteristic specific acoustic impedance z_c and the wave number k differ from those of the free acoustic medium because of viscous and thermal effects at the walls of the hole or tube (6). Define (6)

$$s = r\sqrt{(\omega\rho_0)/\eta}, \tag{4}$$

where r is the radius of the circular hole or tube and ω is the angular frequency. η is the dynamic shear viscosity of the acoustic medium (equal to 1.813×10^{-5} Pa.s for air at 20 °C). The effective density ρ of the acoustic medium in a narrow circular hole or tube due to viscous effects is (6)

$$\rho = \rho_0 \Big/ \left[1 - 2\,\mathrm{J}_1\left(s\sqrt{-j}\right) \Big/ \left\{ s\sqrt{-j}\,\mathrm{J}_0\left(s\sqrt{-j}\right) \right\} \right], \tag{5}$$

where J_0 and J_1 are Bessel functions of the first kind of order 0 and 1 respectively. The effective bulk modulus K of an acoustic medium in a narrow circular hole or tube due to thermal effects is (6)

$$K = \gamma p_0 \Big/ \left[1 + (\gamma - 1)\,2\,\mathrm{J}_1\left(Bs\sqrt{-j}\right) \Big/ \left\{ Bs\sqrt{-j}\,\mathrm{J}_0\left(Bs\sqrt{-j}\right) \right\} \right], \tag{6}$$

where γ is the adiabatic constant of the acoustic medium, p_0 is the ambient pressure of the acoustic medium and B^2 is the Prandtl number of the acoustic medium (equal to 0.71 for air at 20 °C).

The effective normalized characteristic specific acoustic impedance z_c of the acoustic medium in the hole or tube is

$$z_c = \sqrt{K\rho} \,/\, \rho_o c_o. \tag{7}$$

The effective speed of sound c of the acoustic medium in the hole or tube is

$$c = \sqrt{K/\rho}\ . \tag{8}$$

The effective wave number k of the acoustic medium in the hole or tube is

$$k = \omega/c\ . \tag{9}$$

It is interesting to note that Maa's (3) lumped parameter theory for the acoustic medium in a hole or tube does not take account of the thermal effects on the effective bulk modulus predicted by equation (6). The reason for this can be seen by making the low frequency approximation of $\tan(kL) = kL$ in Eq. (3) and using Eqs. (9), (8) and (7) to obtain $\rho_o c_o z_2 = j\omega\rho L$. The effective bulk modulus K has disappeared and this equation is exactly Eq. (5) of Maa (3). In other words, because Maa assumed that the air in the hole or tube was incompressible, he did not need to consider the effective bulk modulus.

The perforation factor ϕ_i is the fraction of the area occupied by an acoustic medium in ith planar layer in any plane parallel to and in between the parallel planes 2 and 1 bounding the ith planar layer. In this paper the perforation factor will be constant across each planar layer but may be different for the acoustic media in different layers. The numbering i of the acoustic layers increases in the opposite direction to which the incident planar sound wave is travelling. Continuity of acoustic pressure and acoustic volume velocity at the planar interface between two planar layers means that the normalized specific acoustic impedances z_i on each side of the planar interface satisfy

$$z_{i+1}/\phi_{i+1} = z_i/\phi_i\ . \tag{10}$$

This means that the normalized specific acoustic impedance in an acoustic medium on ith side of the planar interface (this will usually be z_2 in Eq. (1) for the ith planar layer of acoustic medium) is divided by the perforation factor to convert it to the normalized specific acoustic impedance in an acoustic medium on the (i+1)th side of the planar interface which has a perforation factor of 1. If there are two or more acoustic media on the ith side of the planar interface, after this conversion is carried out, their normalized specific acoustic impedances are combined in the usual way by inverting them, summing the inversions and inverting again. This calculated normalized specific acoustic impedance is then multiplied by the perforation factor of the actual acoustic medium to obtain the normalized specific acoustic impedance that plane waves in the actual acoustic medium encounter on the planar interface (z_1 in Eq. (1)) for the (i+1)th planar layer of acoustic medium.

This approach will not work if there is more than one acoustic medium on the (i+1)th side of the planar interface because acoustic media alter the normalized specific acoustic impedance that the other acoustic media experiences (z_1 in Eq. (1) for the (i+1)th planar layer of acoustic medium). In the calculations described in this paper, this case has been approximated by assuming that z_1 in Eq. (1) in equation is zero. This reduces Eq. (1) to Eq. (3). Similar to above, these parallel lumped parameter normalized specific acoustic impedances are converted to impedances for a perforation ratio of 1 and combined by inverting them, summing the inversions and inverting again. The result is then added the normalized specific acoustic impedance on ith side of the planar interface after this impedance is converted to the value for a perforation factor of 1 as described above.

Although this approximation has worked well, it is possible to avoid the approximation. The simplest method appears to be that of Simon (5). The transfer matrix equation relating the sound pressures and acoustic particle velocities at each side of the planar layer, from which Eq. (1) is derived, is converted to an admittance matrix equation for each acoustic medium in the planar layer after taking account of the perforation factor. These admittance matrices are summed and inverted to obtain the transfer matrix for the planar layer which can be used to obtain an equation which is the equivalent of Eq. (1) for the planar layer. A more general approach is to derive transfer matrices and coupling matrices and combine them into a single matrix equation using the transfer matrix method as described in chapter 11 of Allard and Atalla (6).

Consider the case of holes in a perforated panel whose length is extended by sets of tubes of different length into the air cavity behind the perforated panel. If any of the tube lengths are shorter than the depth of the cavity, the tube ends of different length sets of tubes opening into the air cavity will be in different planes. This is no problem if the cavity is partitioned so that only one set of tubes opens into any one sub cavity and the simple calculation method described in this paper can be used. The calculations show that, if the tubes are different enough in length, two low frequency sound absorption coefficient peaks are obtained. This has been confirmed by experiment (7). If the air cavity is not partitioned, experiment and theory show that only one low frequency sound absorption coefficient peak is obtained (2, 7). Simon (5, 7) was able to make the calculations in this case because, as stated in the introduction of this paper, he assumed that the all tubes opened into the air cavity at one

end of the air cavity which is actually not the situation. Zhang (2) was able to make the calculations because, as stated in the introduction of this paper, she assumed the low frequency approximation for the specific acoustic impedance of the air cavity which does not depend on location in the air cavity. In this paper, the specific acoustic impedances at the different planes in the air cavity, where tube ends open into the air cavity were calculated and averaged taking into account the relative perforation ratios of the sets of different length tubes. As discussed above, in this paper, the impedances of the air in the different length tubes were calculated as lumped parameters assuming the tubes encountered zero impedance at their ends and were combined as parallel elements. However low frequencies were not assumed. The full transfer matrix method could probably be used to avoid any approximations in this case, but the approximate methods agree reasonably well with experiment at low frequencies.

End corrections need to be applied to the ends of tubes which open into the air cavity and the external air space. However, because of the length of the tubes considered in this paper are large compared to their internal radii, these end corrections have little effect. The imaginary part of the end correction normalized specific acoustic impedance at one end of a hole or tube of internal diameter d, whose inside diameter is small compared to the wave length of sound, is

$$\mathrm{Im}(z_e) = hd/2\,, \tag{11}$$

where h equals 0.613 for an unflanged tube, 0.821 for a flanged tube, $8/3\pi = 0.849$ for a baffled piston and $\pi/4 = 0.785$ for a circular hole in a baffle. In this paper, the value of h for an unflanged tube has been used for the end of a tube opening into the air cavity and the value of h for a flanged tube has been used for the end of a tube opening into the external air space. Maa's (3) low frequency lumped parameter theory used the value of h for a baffled piston. When making calculations with Maa's theory, this paper changes Maa's value of h to the values of h used in this paper. The real part of the end correction is

$$\mathrm{Re}(z_e) = \sqrt{\omega\rho_0\eta}\,/\,\rho_0 c_0\,. \tag{12}$$

This formula for the real part is only correct for the end of a hole or tube in an infinite baffle. Thus it will not be correct for the tube ends in the air cavity. However, it has been used in that case in the absence of a better formula because as stated above its effect is minimal because of the length of the tubes. Improved formulae for end corrections of holes and tubes which end in a baffle are discussed by Li (8), but are not used in this paper because of their limited effect due to the length of the tubes and the fact that the tube ends do not always end in a baffle.

When the length of the tubes in the cavity are greater than or equal to the air cavity depth, this paper assumes that the tubes are coiled, if need be, so that their ends are at one end of the cavity (but the value of h for an unflanged tube is still used). In this case the air cavity is treated as one cavity when calculating its impedance. When the length of the tubes in the cavity are less than the air cavity depth, this paper assumes that the tubes are straight and perpendicular to the planar layer. It divides the air cavity into two sub cavities at the plane containing the tube ends which open into the air cavity and calculates the impedance of each sub cavity at the plane containing the tube ends before combining their impedances in parallel after correcting for the perforation ratios as described above. The perforation ratio of the sub cavity not containing the tubes is 1. The perforation ratio of the other sub cavity in the no sub cavity case is reduced by the external volume of the tubes in it.

3. EMPIRICAL CORRECTIONS

Taking account of wave motion in the tubes and in the air cavity did predict a number of the high frequency peaks in the experimentally measured sound absorption coefficient and in the real and imaginary parts of the normalized specific acoustic impedance. It was also hoped that taking account of wave motion would increase the predicted sound absorption coefficient above the low frequency peak where the predicted values are much lower than the experimental values. Examination of the predicted and experimental imaginary part of the normalized specific acoustic impedance showed that the sound absorption coefficient was underestimated mainly because the magnitude of predicted imaginary part of the normalized specific acoustic impedance was overestimated except when the impedance was changing sign. It was decided to impose an empirical correction by limiting the maximum value of the magnitude of the predicted imaginary part of the impedance above the frequency

$$f_l = c_0\sqrt{\phi/(DL)}\,/(2\pi)\,, \tag{13}$$

f_l is an estimate of the frequency of the low frequency sound absorption coefficient peak where the

imaginary part of the normalized specific acoustic impedance changes from negative to positive. ϕ is the perforation ratio of the tubes, D is the depth of the air cavity and L is the length of the tubes. The value of the real part of the normalized specific acoustic impedance was also limited to make the calculations agree better with theory. This was done as follows.

$$y_{corr} = \mathrm{sgn}(y)\left(|y|^{-n} + y_{\mathrm{m}}^{-n}\right)^{-1/n}. \tag{14}$$

sgn(y) is the sign function which returns 1, 0 or -1 if its argument y is positive, zero or negative respectively and n is an integer. y_{corr} is the corrected calculated value, y is the original calculated value and y_m is the empirical magnitude limit of the real or imaginary part of the normalized specific acoustic impedance. Because the value of n was chosen to be the even integer 2, the modulus signs are not actually needed for the imaginary part of the normalized specific acoustic impedance. Because the real part of the predicted normalized specific acoustic impedance cannot be negative, the sgn function and the modulus signs are not actually needed for the real part of the impedance. In this paper, y_m has been set to 15 for the imaginary part of the normalized specific acoustic impedance and to 45 for the real part of the normalized specific acoustic impedance. This correction only needs to be applied to the imaginary part of the normalized specific acoustic impedance when Maa's lumped parameter model is used for the tubes.

The second empirical correction made in this paper applies to the wave number in the air cavity. The real part of this wave number has, as is usual, been set equal to the wave number of sound in free air. To control the magnitude of resonances in the air cavity, the imaginary part of the wave number in the air cavity has been changed from 0 to -0.2. To make the predicted frequency at which the low frequency sound absorption coefficient peak occurs agree better with experiment, the internal diameters of the two tubes were increased by 0.1 mm.

4. EXPERIMENTS

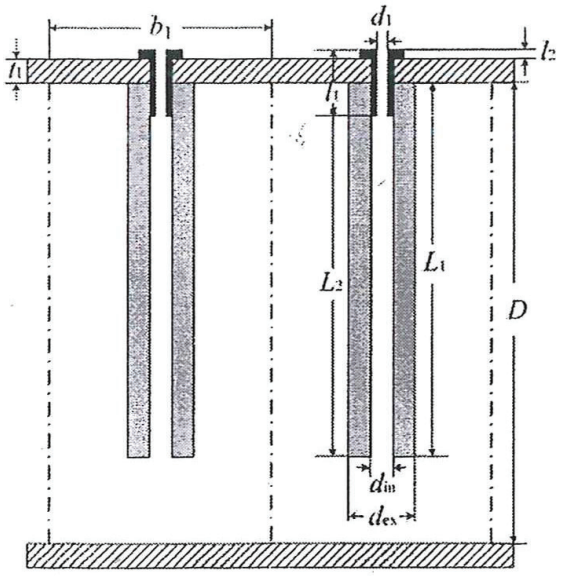

Figure 1. The sound absorbing system studied in this paper. This is Fig. 2.1(a) of Zhang (2).

The sound absorbing system studied in this paper is shown in Fig. 1. The system consists of a perforated plate of thickness t_1 = 2 mm with the holes arranged in a square array with the sides of the squares having a length of b_1 = 4.8 mm. Copper ferules with an internal diameter of d_1 = 1.1 mm and a total length of l_1 = 9.3 mm fill the holes in the perforated plate and their narrow flanges stand l_2 = 0.2 mm above the perforated plate. Rubber tubes with an internal diameter of d_{in} = 1. 2 mm, an external diameter of d_{ex} = 2.6 mm and a length of L_1 are inserted over the length of the copper ferules in the air cavity. The air cavity has a depth of D = 43 or 120 mm. L_1 varied in 10 mm steps from 10 mm to 80 for the 43 mm deep air cavity or to 160 mm for the 120 mm deep air cavity. Measurements were also made when b_1 = 7 mm for L_1 equals 20, 40 or 80 mm when D =43 or 120 mm. Each tube system consists of two tubes in series. The first, in the direction of exiting the air cavity, is a tube with an internal

diameter of d_{in} = 1. 2 mm and a length of $L_2 = L_1 + t_1 + l_2 - l_1$. The second is a tube of internal diameter of d_1 = 1.1 mm and a length of l_1 = 9.3 mm. Zhang (2) also made measurements with half of the rubber tubes having a length of 10, 20 or 40 mm while the other half of the rubber tubes had a length 80 mm for a cavity depth of D = 43 or 120 mm.

Zhang (2) made the measurements using a two microphone impedance tube with an internal square cross section of 40 x 40 mm and a length of 1.2 m between the face of the specimen and loudspeaker. To avoid cross modes, the maximum frequency must be less than 4295 Hz. The maximum measurement frequency of 3200 Hz is well below this limit. The distance of the closest microphone to the face of the sample was 268 mm. The low and high frequency measurements were made with the two microphones spaced 150 mm and 50 mm apart respectively. ISO 10534-2 (9) requires that the maximum frequency be 10 % less than the frequency at which the microphone spacing is equal to half the wave length of sound. Thus the low and high frequency measurement maximum frequencies are 1031 and 3093 respectively. However in this paper, the experimental results have been graphed up to 3200 Hz. This was done because it was observed that apart from when one of the microphone spacings was close to a multiple of half the wave length of the sound, the high and low frequency measurements agreed reasonably well. It should be noted that when the microphone spacing is close to a multiple of half the wave length of the sound which occurs at 1145, 2290 and 3436 Hz, the measurement uncertainty becomes very large.

ISO 10534-2 (9) says that "The lower frequency limit is dependent on the spacing between the microphones and the accuracy of the analysis system but, as a general guide, the microphone spacing should exceed 5 % of the wavelength corresponding to the lower frequency of interest." Thus the recommended minimum measurement frequencies for the low and high frequency measurements are 115 and 345 Hz respectively. However, because some of the frequencies at which sound absorption coefficient peaks occur are below these frequencies, measurements down to 50 Hz have been graphed. It should be noted that the measurement uncertainty increases below the recommended minimum measurement frequencies.

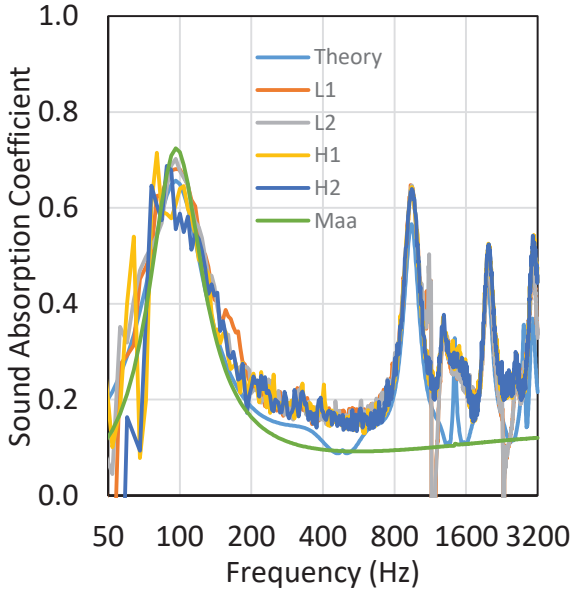

Figure 2. The normal incident sound absorption coefficient of a system with 160 mm long rubber tubes in a 120 mm deep air cavity.

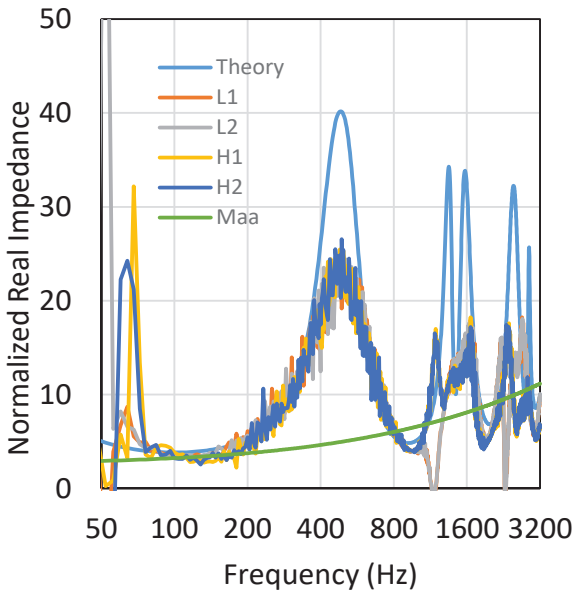

Figure 3. The real part of the normalized specific acoustic impedance of a system with 160 mm long rubber tubes in a 120 mm deep air cavity.

When the spacing between the centres of the closest perforations was b_1 = 4.8 mm, there were 64 perforations in the 40 by 40 mm front perforated panel in an 8 by 8 square array. Had the holes been spaced equally across the whole of the 40 mm in each direction, b_1 would have been 5 mm. Thus the question arose whether it was better to calculate the average perforation ratio across the whole of the front perforated panel by assuming that b_1 = 5 mm or use the perforation ratio of the holes near the centre of the front perforated panel by using b_1 = 4.8 mm. Comparison of the predicted frequency at which the low frequency sound absorption coefficient peak occurs with the experimental value showed

that b_1 = 4.8 mm was a better choice.

5. COMPARISON OF THEORY WITH EXPERIMENT

For each sound absorbing system, Zhang (2) made two low frequency measurements, L1 and L2, and two high frequency measurements, H1 and H2. Zhang averaged the two low frequency measurements together and averaged the two high frequency measurements together. She joined the measurements in the two different frequency ranges together by averaging these two averages in an overlapping frequency range in which they were both valid. However in this paper, all four measurement results are displayed to give an indication of the measurement uncertainty. Note that the departure of the low frequency measurements from the high frequency measurements for frequencies near 1145 and 2290 Hz is due to the low frequency measurement microphone spacing being close to a multiple of half the wavelength of sound.

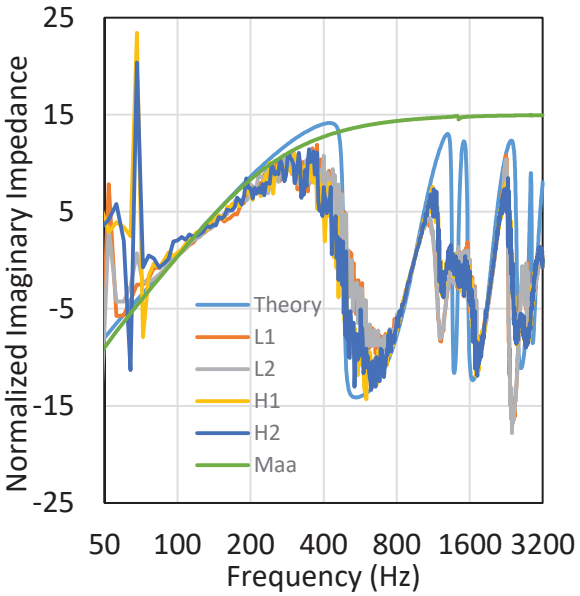

Figure 4. The imaginary part of the normalized specific acoustic impedance of a system with 160 mm long rubber tubes in a 120 mm deep air cavity.

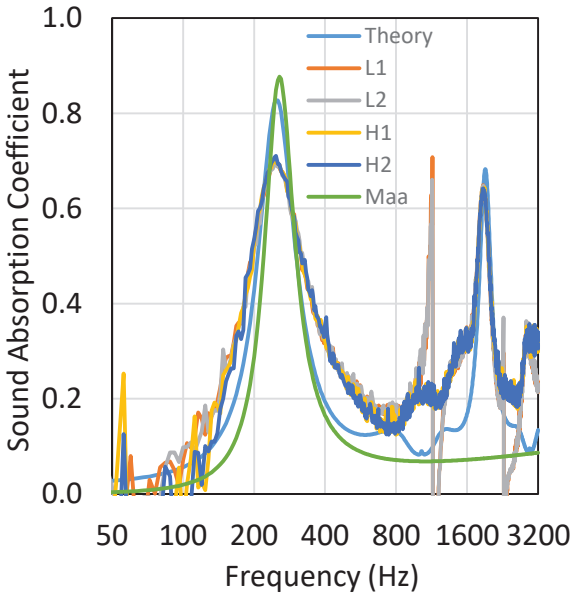

Figure 5. The normal incident sound absorption coefficient of a system with 80 mm long rubber tubes in a 43 mm deep air cavity.

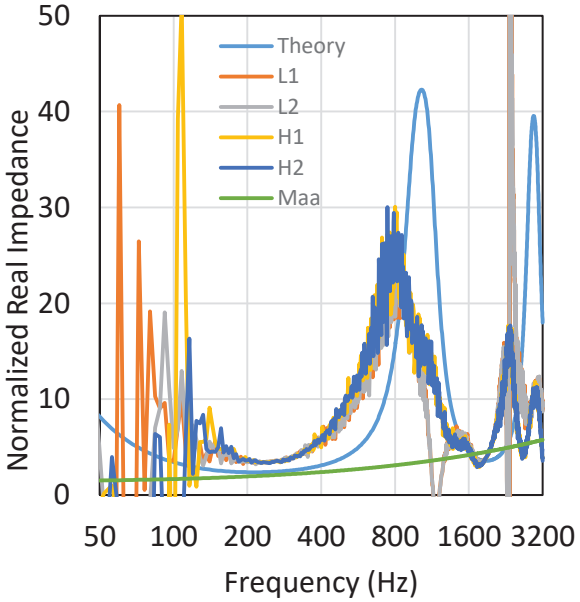

Figure 6. The real part of the normalized specific acoustic impedance of a system with 80 mm long rubber tubes in a 43 mm deep air cavity.

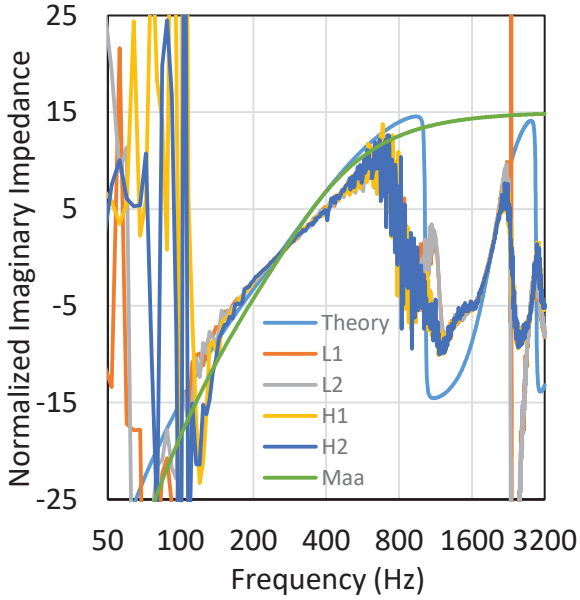

Figure 7. The imaginary part of the normalized specific acoustic impedance of a system with 80 mm long rubber tubes in a 43 mm deep air cavity.

Figs. 2 to 7 compare the four measurement results with the theory described in this paper and with the theory when Maa's lumped parameter model is used for the two tubes for a cavity depth of 120 mm with 160 mm long rubber tubes and for a cavity depth of 43 mm with 80 mm long rubber tubes. The sound absorption coefficient and the real and imaginary parts of the normalized specific acoustic impedance are shown. Both the theory described in this paper and Maa's theory are able to predict the low frequency sound absorption coefficient peak, but only the theory described in this paper is able to predict the higher frequency peaks. The theory described in this paper is able to predict the frequency of the sound absorption coefficient peaks but does not always predict the amplitude of these peaks as accurately as would be desired. The empirical corrections adopted in this paper have increased the predicted sound absorption coefficients between the peaks so that these predicted values are closer to the experimentally measured values. The empirical corrections have also brought the predicted real and imaginary parts of the normalized specific acoustic impedance closer to the experimental values.

6. CONCLUSIONS

Modelling the wave motion in the air in the bore of long tubes, rather than modelling this air as a lumped parameter, enables the prediction of the frequencies of the higher frequency sound absorption coefficient peaks although the prediction of the amplitude of these peaks is not always as accurate as would be desired. However, the modelling of this wave motion was not sufficient to increase the predicted values of the sound absorption coefficient at frequencies between the frequencies of the peaks so that the predicted values were closer to the experimental values. It was necessary to impose limits on the values of the real and imaginary parts of the normalized specific acoustic impedance in order to increase these predicted values of the sound absorption coefficient. The imaginary part of the wave number in the air cavity was also empirically set to a non-zero value in order to remove predicted spikes due to cavity resonances.

ACKNOWLEDGEMENTS

The authors acknowledge the financial support provided by the Chinese Academy of Sciences (CAS) and CSIRO which enabled the first author to make a two week CAS-CSIRO Exchange visit to The Key Laboratory of Noise and Vibration Research, Institute of Acoustics, Chinese Academy of Sciences in Beijing in the second half of May 2018 which resulted in this paper.

REFERENCES

1. Lyu Y, Li X, Tian J, Wei W. The perforated panel resonator with flexible tube bundle and its acoustical measurements. Inter-noise 2001; 27-30 August 2001; The Hague, The Netherlands: I-INCE; 2001. p. 1-4.
2. Zhang Q. Investigation on sound absorption characteristics of perforated panel resonator with tube bundles and with built-in resonators [PhD]. Beijing, China: Graduate University of Chinese Academy of Sciences; 2011.
3. Maa D. Theory and design of microperforated panel sound absorbing constructions. Scientia Sincia. 1975;18(1):55-71.
4. Larner DJ, Davy JL. Predicting the Absorption of Perforated Panels Backed by Resistive Textiles. Noise Control Engineering Journal. 2016;64:259-67.
5. Simon F. Long Elastic Open Neck Acoustic Resonator for low frequency absorption. Journal of Sound and Vibration. 2018;421:1-16.
6. Allard JF, Atalla N. Propagation of Sound in Porous Media: Modelling Sound Absorbing Materials. 2nd ed. Chichester, UK: John Wiley & Sons; 2009. 1-358 p.
7. Simon F. Long elastic open neck acoustic resonator in flow. Inter-noise 2016; 21-24 August 2016; Hamburg, Germany: I-INCE; 2016. p. 1-12.
8. Li X. End correction model for the transfer impedance of microperforated panels using viscothermal wave theory. Journal of the Acoustical Society of America. 2017;141(3):1426-36.
9. International Organization for Standardization. ISO 10534-2:1998(E) Acoustics — Determination of sound absorption coefficient and impedance in impedance tubes — Part 2: Transfer-function method. 1998. p. 1-27.